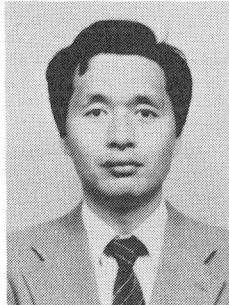


EXPERIMENTAL STUDIES ON SEISMIC DESIGN OF A PIER  
WITH REINFORCEMENT TERMINATED HALFWAY IN A TENSION ZONE

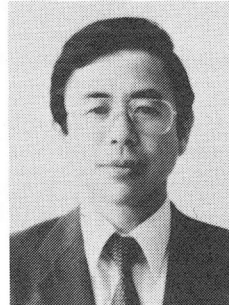
(Translation from Proceeding of JSCE, No.348/V-1, August 1984)



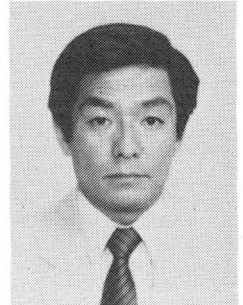
Tsuyoshi YAMAMOTO



Tadayosi ISHIBASHI



Masayuki OTSUBO



Shinji KOBAYASHI

SYNOPSIS

In the case of pier structures, reinforcing bars are cut off and terminated halfway. As a result, the cutoff bars are resulted to be terminated in a tension zone of members. According to the past records of earthquakes, some pier structures had been damaged near the cutoff zones.

This paper describes as follows :

1. An experimental study on the behavior of pier specimens with cutoff zone under alternate cyclic lateral loading.
2. Some rational proposal on the seismic design method for cutoff zone in pier structure.

On the basis of the results, flexural strength of cutoff zone will be raised to a level equivalent to the root of pier. Thereby, the resisting moment strength is improved to 1.5 times that of design moment at cutoff zone.

---

T. Yamamoto is a general manager at Structural Design Office of the Japanese National Railways (JNR), Japan. He is a member of JSCE and JCI.

---

T. Ishibashi is a chief research engineer at Structural Design Office of the Japanese National Railways (JNR), Japan. He is a member of JSCE and JCI.

---

M. Otsubo is a chief engineer at Osaka Construction Bureau of the Japanese National Railways (JNR), Japan. He is a member of JSCE and JCI.

---

S. Kobayashi is a chief constructor at Hiroshima Branch Office, Shimizu Construction Co., Ltd., Japan. He is a member of JSCE and JCI.

---

## 1. INTRODUCTION

In the case of pier structures, the portion of longitudinal reinforcing bars is usually cut off and terminated halfway since the cutoff bars are theoretically not required to resist to flexure and such a practice is economical. However, the cutoff bars become in a tension zone on the loading. In principal, flexural reinforcement should not be terminated in a tension zone. Actually, damages of piers occurred mostly at cutoff zone, for example, in the case of the earthquake off Miyagi Prefecture in June 1978 and that off Uraga in March 1982.

Therefore, alternate loading tests on pier specimens with a cutoff point were conducted in order to investigate the strength and displacement behavior of pier structures under a seismic load.

This paper reports these test results and proposes a rational design method at cutoff zone of pier structures under a seismic load.

## 2. EVALUATION OF THE EARTHQUAKE-PROOF OF REINFORCED CONCRETE MEMBERS

When an elasto-plastic structure such as reinforced concrete member is subjected to a seismic load, such a member indicates a load-displacement envelope curve as shown by the curve OAB in Fig. 1. On the other hand, when the same seismic load is applied in a perfect elastic structure which has the same rigidity as the yield rigidity of the above elasto-plastic structure, its response indicates the line OAE in Fig. 1. In this case, it is known that an energy conservation rule where Area  $\triangle OED$  = Area  $\triangle OABC$  is applied.<sup>1)</sup> So that, it is possible to evaluate the earthquake-proof capacity of an elasto-plastic structure as the response of the equivalent elastic structure. In other words, the larger the deformation capacity of the elasto-plastic structure, the more the structure will be resistant to earthquakes. In this report, the earthquake-proof capacity of reinforced concrete piers is also evaluated on the basis of the above concept.

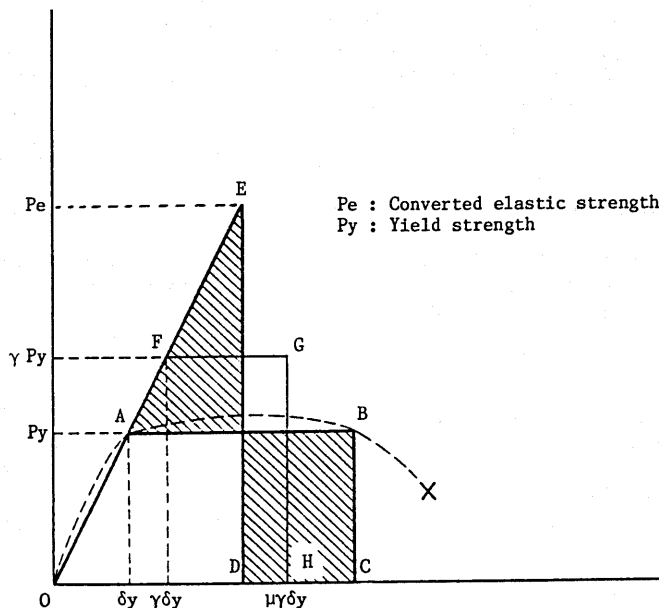


Fig. 1 Typical load-displacement curve

### 3. EXPERIMENTAL STUDY ON ALTERNATE LOADING OF PIER WITH REINFORCING BARS TERMINATED IN A TENSION ZONE

#### (1) Scope

##### a) Variables in test specimens

The dimensions of the test specimens are shown in Table 1. This experiment was conducted by focusing mainly on the following variables: Namely, for Series I, M/Sd at cutoff point, ratio of tension reinforcement  $A_s/bd$  at cutoff point, cutoff ratio (ratio of area of cutoff bars to total area of cutoff bars and non-cutoff bars at cutoff point), ratio of shear reinforcement  $A_w/b_s$ , and axial force  $N/bh$ ; for Series II, ratio of shear reinforcement and M/Sd; and for Series III, ratio of shear reinforcement  $A_w/D_s$ , axial force  $4N/\pi D^2$  and characteristics of circular pier specimens. where

- M: bending moment at cutoff point  
S: shear force at cutoff point  
d: effective depth  
D: diameter of circular pier specimen

Table 1 Properties of Specimens

| Specimen                  |                        | Thick-<br>ness | Width     | Height |       | Cutoff<br>ratio |     | ratio of<br>reinforcement |           | Axial force |           | Dia-<br>meter<br>of<br>rebar | Calculated strength at Cutoff point |              |                |                           |       |                      |
|---------------------------|------------------------|----------------|-----------|--------|-------|-----------------|-----|---------------------------|-----------|-------------|-----------|------------------------------|-------------------------------------|--------------|----------------|---------------------------|-------|----------------------|
| Shape                     | No.                    |                |           |        |       |                 |     | h<br>(cm)                 | b<br>(cm) | H<br>(cm)   | a<br>(cm) |                              | M/Sd                                | P $\rho$ (%) | P $\omega$ (%) | (kg/<br>cm <sup>2</sup> ) | (MPa) | Yield<br>strength Sy |
|                           |                        |                |           |        |       |                 |     |                           |           |             |           |                              | (tf)                                | (kN)         | (tf)           | (kN)                      | (tf)  | (kN)                 |
| Rectangular pier specimen | I - 1                  | 35             | 150       | 200    | 150   | 1/3             | 4.8 | 0.68                      | 0         | 10          | 0.98      | D13                          | 25.9                                | 253.8        | 26.6           | 260.7                     | 28.5  | 279.3                |
|                           | 2                      | 35             | 150       | 200    | 150   | 1/2             | 4.8 | 0.52                      | 0         | 10          | 0.98      | "                            | 21.1                                | 206.8        | 21.7           | 212.7                     | 27.2  | 266.7                |
|                           | 3                      | 35             | 150       | 200    | 112.5 | 1/2             | 3.6 | 0.52                      | 0.17      | 10          | 0.98      | "                            | 28.1                                | 275.4        | 28.9           | 283.2                     | 51.4  | 503.7                |
|                           | 4                      | 35             | 150       | 200    | 112.5 | 1/2             | 3.6 | 0.52                      | 0         | 0           | 0         | "                            | 21.8                                | 213.6        | 22.5           | 220.5                     | 23.1  | 226.4                |
|                           | 5                      | 35             | 150       | 200    | 112.5 | 1/2             | 3.6 | 0.52                      | 0.17      | 0           | 0         | "                            | 21.8                                | 213.6        | 22.5           | 220.5                     | 47.3  | 463.5                |
|                           | 6                      | 35             | 150       | 100    | 50    | 1/2             | 1.6 | 0.35                      | 0         | 0           | 0         | "                            | 34.0                                | 333.2        | 35.4           | 346.9                     | 20.2  | 198.0                |
|                           | 7                      | 35             | 150       | 100    | 50    | 1/2             | 1.6 | 0.35                      | 0.15      | 0           | 0         | "                            | 34.0                                | 333.2        | 35.4           | 346.9                     | 41.6  | 407.7                |
|                           | 8                      | 35             | 150       | 150    | 100   | 1/2             | 3.2 | 0.35                      | 0.15      | 10          | 0.98      | "                            | 24.2                                | 237.2        | 25.5           | 249.9                     | 46.9  | 459.6                |
|                           | 9                      | 35             | 150       | 150    | 112.5 | 1/2             | 3.6 | 0.35                      | 0         | 0           | 0         | "                            | 15.1                                | 148.0        | 15.9           | 155.8                     | 20.2  | 198.0                |
|                           | 10                     | 35             | 150       | 150    | 75    | 1/2             | 2.4 | 0.35                      | 0         | 0           | 0         | "                            | 22.7                                | 222.5        | 23.9           | 234.2                     | 20.2  | 198.0                |
|                           | 11                     | 35             | 150       | 150    | 112.5 | 1/2             | 3.6 | 0.35                      | 0.15      | 0           | 0         | "                            | 15.1                                | 148.0        | 15.9           | 155.2                     | 41.6  | 407.7                |
|                           | 12                     | 35             | 150       | 150    | 75    | 1/2             | 2.4 | 0.35                      | 0.15      | 0           | 0         | "                            | 22.7                                | 222.5        | 23.9           | 234.2                     | 41.6  | 407.7                |
| Rectangular pier specimen | II - 2                 | 60             | 60        | 130    | 80    | 1/2             | 1.5 | 0.66                      | 0.63      | 10          | 0.98      | D16                          | 61.9                                | 606.6        | 64.0           | 627.2                     | 81.9  | 802.6                |
|                           | 3                      | 60             | 60        | 130    | 80    | 1/2             | 1.5 | 0.66                      | 0         | 10          | 0.98      | "                            | 61.9                                | 606.6        | 64.0           | 627.2                     | 18.2  | 178.4                |
|                           | 4                      | 60             | 60        | 130    | 80    | 1/2             | 1.5 | 0.23                      | 0.27      | 10          | 0.98      | D13                          | 29.0                                | 284.2        | 30.5           | 298.9                     | 42.6  | 417.5                |
|                           | 5                      | 60             | 60        | 130    | 80    | 1/2             | 1.5 | 0.23                      | 0         | 10          | 0.98      | "                            | 29.0                                | 284.2        | 30.5           | 298.9                     | 15.3  | 149.9                |
|                           | 6                      | 40             | 60        | 95     | 52.5  | 1/2             | 1.5 | 1.13                      | 0.99      | 10          | 0.98      | D16                          | 59.5                                | 583.1        | 60.6           | 593.9                     | 78.9  | 773.2                |
|                           | 7                      | 40             | 60        | 155    | 87.5  | 1/2             | 2.5 | 2.02                      | 0.63      | 10          | 0.98      | D22                          | 60.8                                | 595.8        | 61.9           | 606.6                     | 59.1  | 579.2                |
|                           | 8                      | 40             | 60        | 155    | 87.5  | 1/2             | 2.5 | 1.23                      | 0.36      | 10          | 0.98      | D19                          | 38.6                                | 378.2        | 39.3           | 385.1                     | 41.7  | 409.0                |
|                           | 9                      | 40             | 60        | 155    | 87.5  | 1/2             | 2.5 | 0.54                      | 0.27      | 10          | 0.98      | D13                          | 19.5                                | 191.1        | 20.1           | 197.0                     | 30.0  | 294.0                |
|                           | 10                     | 40             | 60        | 155    | 87.5  | 1/2             | 2.5 | 0.54                      | 0.27      | 10          | 0.98      | "                            | 19.5                                | 191.1        | 20.1           | 197.0                     | 30.0  | 294.0                |
|                           | Circular pier specimen | III-15         | $\phi$ 65 |        | 165   | 97.5            | 1/2 | 1.5                       | 0.13      | 0.25        | 10        | 0.98                         | D13                                 | 21.5         | 210.7          | 25.6                      | 250.9 | 37.7                 |
| 16                        |                        | $\phi$ 65      |           | 165    | 97.5  | 1/2             | 1.5 | 0.41                      | 0.63      | 10          | 0.98      | D22                          | 45.9                                | 449.8        | 54.6           | 535.1                     | 79.3  | 777.1                |
| 17                        |                        | $\phi$ 65      |           | 165    | 97.5  | 1/2             | 1.5 | 0.30                      | 0.63      | 20          | 1.96      | D19                          | 43.0                                | 421.4        | 50.1           | 491.0                     | 79.8  | 782.0                |
| 18                        |                        | $\phi$ 65      |           | 230    | 162.5 | 1/2             | 2.5 | 0.45                      | 0.25      | 10          | 0.98      | D22                          | 25.3                                | 247.9        | 29.0           | 284.2                     | 40.0  | 392.0                |
| 19                        |                        | $\phi$ 65      |           | 230    | 162.5 | 1/2             | 2.5 | 0.18                      | 0.25      | 20          | 1.96      | D16                          | 20.1                                | 197.0        | 22.6           | 221.5                     | 40.1  | 393.0                |
| 20                        |                        | $\phi$ 65      |           | 230    | 162.5 | 1/2             | 2.5 | 0.18                      | 0.13      | 20          | 1.96      | "                            | 20.1                                | 197.0        | 22.6           | 221.5                     | 27.9  | 273.4                |

- $A_s$ : area of tension reinforcement in rectangular pier specimen  
 $A_s'$ : a quarter of area of tension reinforcement in circular pier specimen  
 $A_w$ : area of shear reinforcement within a distance  $s$   
 $N$ : axial force  
 $h$ : overall thickness of member in rectangular pier specimen  
 $b$ : width of member in rectangular pier specimen

Meanwhile, since cutoff ratio in actual piers is generally  $1/2$ , cutoff ratio was compared with respect to  $1/2$  and  $1/3$  in this experiment.

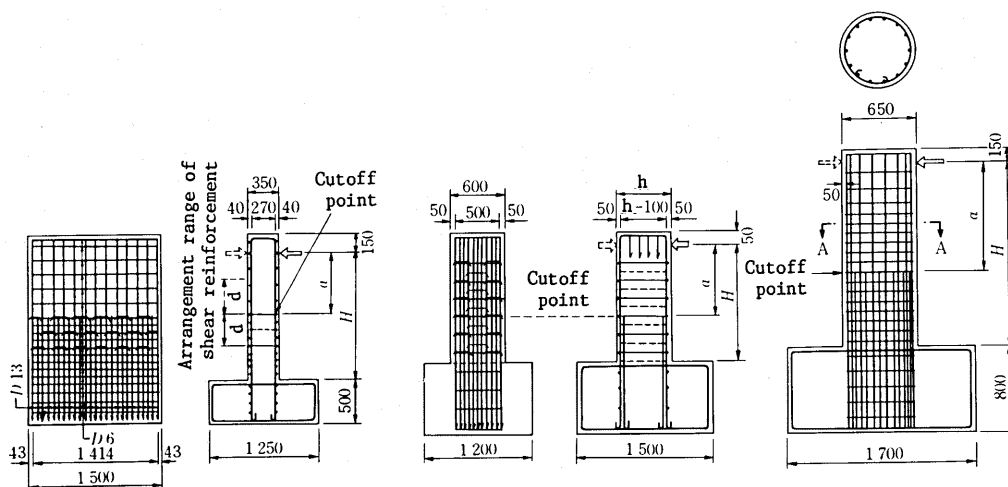
#### b) Arrangement of reinforcement

Typical arrangements of reinforcement are shown in Fig. 2. The arrangements were so determined that the reinforcement at cutoff point would reach yield earlier than the reinforcement at the root of pier specimen. Moreover, the distance from the root to cutoff point was made greater than either of the development length  $30\phi$  ( $\phi$ : diameter of reinforcement) or effective depth  $d$  ( $D$  in the case of circular pier specimen), since the failure characteristics at cutoff zone should have no effect on the behavior of the root of pier specimen. Therefore, in the case of II-2 through II-5, the distance was made by 5 cm smaller than  $d$  in order to make the flexural strength at the root larger than that at cutoff point.

Shear reinforcements at cutoff zone were arranged respectively in a range of upper and lower  $d$ , except in the case of I-11 and I-12 where shear reinforcements at cutoff zone were arranged in a range of lower  $d$ .

All shapes of shear reinforcements were of a closed type.

The longitudinal reinforcements were arranged in two stages for II-2, II-3 and II-6 through II-10, and all of the second stage (inside) reinforcing bars were cut off. The other specimens have one stage of longitudinal reinforcement. Moreover, for II-5 and II-10, the cutoff bars were bent and terminated rectangularly toward inside the specimens.



(a) Series I

(b) Series II

(c) Series III

Fig. 2 Typical specimens



### c) Strength of specimens

The calculated strengths of specimens are shown also in Table 1. The values were obtained by using the strength of actual materials given below.

Reinforcement (SD30 in Japanese Industrial Standard)

$F_{sy} = 4,000 \text{ kgf/cm}^2$  (392 MPa),  $F_{su} = 5,400 \text{ kgf/cm}^2$  (529 MPa),

$E_s = 2.1 \times 10^6 \text{ kgf/cm}^2$  ( $0.206 \times 10^6 \text{ MPa}$ ),

$A_s$  (actual area estimated based on the results of tensile strength tests of reinforcements): 1.14  $\text{cm}^2$  for D13

1.86  $\text{cm}^2$  for D16

2.72  $\text{cm}^2$  for D19

3.72  $\text{cm}^2$  for D22

Concrete

Compressive strength( $F_c'$ ): 200  $\text{kgf/cm}^2$  (19.6 MPa) for Series I

260  $\text{kgf/cm}^2$  (25.5 MPa) for Series II

300  $\text{kgf/cm}^2$  (29.4 MPa) for Series III

The calculated values of flexural yield strength of specimens are those when tension reinforcements reached yield. (In the case of circular pier specimen, the reinforcements at the position indicated in Fig. 3 reached yield.)

Meanwhile, the calculated values of flexural ultimate strength of specimen were based upon the Structural Design Standards of the Japanese National Railways (JNR).<sup>2)</sup> And, the calculated values of shear strength of specimens were based upon the Eq.(1).<sup>3)</sup>

$$V_y = 0.94(F_c')^{1/3} (1 + \beta_d + \beta_p + \beta_n) b \cdot d$$

$$+ A_w \cdot F_{sy} \cdot z (\sin \alpha + \cos \alpha) / s \dots \dots \dots (1)$$

$$\left[ V_y = 0.20(F_c')^{1/3} (1 + \beta_d + \beta_p + \beta_n) b \cdot d \right.$$

$$\left. + A_w \cdot F_{sy} \cdot z (\sin \alpha + \cos \alpha) / s \text{ ----( SI unit )} \right]$$

$$\beta_d = \sqrt[4]{100/d} - 1$$

$$\beta_p = \sqrt{100 \cdot p_1} - 1 \leq 0.73$$

$$\beta_n = 2 \cdot M_o / M_u$$

Where  $V_y$ : shear strength

$F_c'$ : compressive strength of concrete

$d$ : effective depth (D in the case of circular pier specimen)

$p_1$ : ratio of tension reinforcement ( $4 A_s' / \pi D^2$  in the case of circular pier specimen)

$M_o$ : moment at the limit of inducing tensile stress in a section

$M_u$ : moment strength

$A_w$ : area of shear reinforcement within a distance  $s$

$F_{sy}$ : yield strength of shear reinforcement

$\alpha$ : angle between shear reinforcement and longitudinal axis of member

$z$ : 0.875d

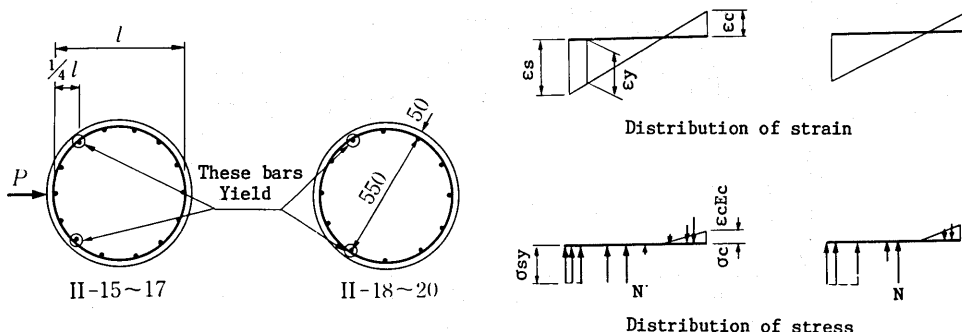


Fig. 3 Assumption for calculating flexural yield strength of circular pier

## (2) Method of experiment

The followings were observed : applied loads, horizontal displacements, strains of longitudinal reinforcements and shear reinforcements, crack widths, etc. For Series II and III, the vertical displacements at the top of specimen were also measured. Meanwhile, the strains of longitudinal reinforcements in footing for Series I were measured to investigate slip-out of reinforcement from footing. However, in the test results, such slip-out was not caused since yield of reinforcement at cutoff point was predominant and the strain in footing showed almost no change at each displacement level. Therefore, for Series II and III, such strains in footing were not measured. The loads were applied in a lateral direction by a hydraulic jack which was controlled in a displacement mode. Specimens were subjected to alternately cyclic loading with 10 cycles at each displacement level. The displacement level was increased incrementally as  $\delta y$ ,  $2\delta y$ ,  $3\delta y$ .  $\delta y$  was defined as the displacement at load position when the tension reinforcement at cutoff point reached yield in rectangular pier specimens. (in the circular pier specimens, when the reinforcing bars at specified position at cutoff point reached yield. Specified position is about one-fourth the diameter of a circle formed by connecting the center of reinforcing bars from the reinforcing bar on the tension edge side, as shown in Fig 3.) However, when the peak value of load at third cycle at each displacement level became greater than 95% of the peak value of load at second cycle, specimens were subjected to alternately cyclic loading at the subsequent displacement level. The axial force was provided by using PC steel bars for Series I. However, for Series II and III, in order that PC steel bars have an effect on evaluation of the ductility and that a constant axial force would be provided regularly in the vertical direction, the axial force was provided by a hydraulic jack system with a pantagraph and a rotary disk.

## (3) Results of experiments

Table 2 shows the yield load  $P_o$ , maximum load  $P_{max}$ , the ratio of these loads to calculated values, and ductility factor of each specimen.

Fig. 4 shows typical load-displacement envelope curves at positive and negative loading, and the lower limit envelope curve. The symbols in Fig. 4 mean as

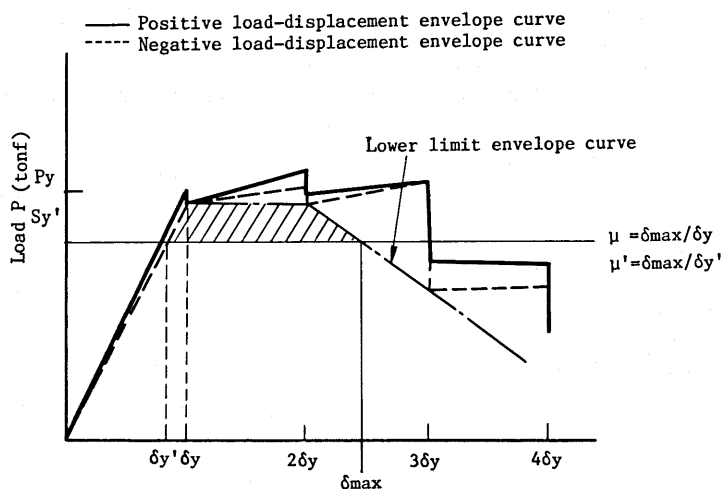


Fig. 4 Method of calculating the ductility factor

follows :  $S_y'$  is calculated the flexural yield load calculated as disregard of cutoff bars in the section where locates at the larger distance of effective depth or development length below cutoff point.  $P_y$  is the flexural yield load and  $\delta_y$  is the yield displacement.  $\delta_y'$  and  $\delta_{max}$  are the lower value and the upper value of the displacements of the lower limit envelope curve at  $S_y'$ . The ductility factor  $\mu$  was obtained by dividing the maximum displacement  $\delta_{max}$  by the yield displacement  $\delta_y$ . And the ductility factor  $\mu'$  was obtained by dividing the maximum displacement  $\delta_{max}$  by  $\delta_y'$  instead of  $\delta_y$ . Meanwhile, in the case of circular pier specimen, the methods of calculating flexural yield strength and shear strength are yet to be established. Therefore, for this experiment, as shown in Fig 3, flexural yield strength was defined to be reached when the reinforcing bar at the position about one-fourth the diameter of a circle formed by connecting the center of bars reached yield. And then, shear strength was calculated according to Eq. (1).

#### a) Displacement

Typical load-displacement curves are shown in Fig. 5, where the displacement means the horizontal displacement at load position. The horizontal displacement was measured at intervals of 20 cm through 30 cm from the root of pier through to its top.

Table 2 The results of experiment and comparison with calculated values

| Specimen                  |        | Yield load |         | Maximum load |         | Ductility factor |        | Proportion to cal. value |        |        | Failure by            |
|---------------------------|--------|------------|---------|--------------|---------|------------------|--------|--------------------------|--------|--------|-----------------------|
| Shape                     | No.    | Po(tonf)   | Po(kN)  | Pm(tonf)     | Pm(kN)  | $\mu$            | $\mu'$ | Po/Sy                    | Pm/Su  | Po/Vy  |                       |
| Rectangular pier specimen | I-1    | 25.7       | 251.9   | 27.0         | 264.6   | 2.5              | 2.6    | 0.99                     | 1.02   | 0.90   | Yield at cutoff point |
|                           | 2      | 21.7       | 212.7   | 23.3         | 228.3   | 2.6              | 3.0    | 1.03                     | 1.07   | 0.80   | "                     |
|                           | 3      | 26.5       | 259.7   | 29.9         | 293.0   | 2.5              | 3.0    | 0.94                     | 1.03   | 0.52   | "                     |
|                           | 4      | 22.4       | 219.5   | 22.4         | 219.5   | 1.3              | 1.8    | 1.03                     | 1.00   | 0.97   | "                     |
|                           | 5      | 20.6       | 201.9   | 22.7         | 222.5   | 2.5              | 3.1    | 0.94                     | 1.01   | 0.44   | "                     |
|                           | 6      | 28.4       | 278.3   | 28.4         | 278.3   | 2.0              | 2.8    | 0.94                     | 0.80   | 1.41   | "                     |
|                           | 7      | 29.7       | 291.1   | 29.7         | 291.1   | 3.0              | 3.9    | 0.87                     | 0.84   | 0.71   | "                     |
|                           | 8      | 23.5       | 230.3   | 27.2         | 266.6   | 3.2              | 3.9    | 0.97                     | 1.07   | 0.50   | "                     |
|                           | 9      | (16.4)     | (160.7) | (18.4)       | (180.3) | —                | —      | (1.09)                   | (1.16) | (0.81) | "                     |
|                           | 10     | 21.6       | 211.7   | 22.0         | 215.6   | 3.0              | 3.3    | 0.95                     | 0.92   | 1.07   | "                     |
|                           | 11     | 14.0       | 137.2   | 16.5         | 161.7   | > 4              | > 4.6  | 0.93                     | 1.04   | 0.34   | "                     |
|                           | 12     | 21.1       | 206.8   | 22.9         | 224.4   | > 4              | > 5.2  | 0.93                     | 0.96   | 0.51   | "                     |
| Rectangular pier specimen | II-2   | 45.3       | 443.9   | 57.1         | 559.6   | > 4              | > 4.8  | 0.73                     | 0.89   | 0.55   | Yield at cutoff point |
|                           | 3      | 43.0       | 421.4   | 43.0         | 421.4   | < 1              | < 1    | 0.69                     | 0.67   | 2.36   | "                     |
|                           | 4      | 27.0       | 264.6   | 28.5         | 279.3   | 3.5              | 4.0    | 0.93                     | 0.93   | 0.63   | "                     |
|                           | 5      | 25.3       | 247.9   | 25.3         | 247.9   | 1.1              | 1.3    | 0.87                     | 0.83   | 1.65   | "                     |
|                           | 6      | 40.8       | 399.8   | 51.1         | 500.8   | 3.4              | 3.7    | 0.69                     | 0.84   | 0.52   | "                     |
|                           | 7      | 49.5       | 485.1   | 50.7         | 496.9   | 1.4              | 1.7    | 0.81                     | 0.82   | 0.50   | "                     |
|                           | 8      | 29.8       | 292.1   | 32.6         | 319.5   | 2.4              | 2.9    | 0.77                     | 0.83   | 0.71   | "                     |
|                           | 9      | 17.0       | 166.6   | 19.5         | 191.1   | 2.6              | 2.7    | 0.87                     | 0.97   | 0.57   | "                     |
|                           | 10     | 17.5       | 171.5   | 18.6         | 182.3   | —                | —      | —                        | —      | —      | Yield at root         |
|                           | 10R    | 17.4       | 170.5   | 20.2         | 198.0   | 2.5              | 2.9    | 0.89                     | 1.00   | 0.58   | Yield at cutoff point |
| Circular pier specimen    | III-15 | 20.7       | 202.9   | 25.1         | 246.0   | 3.7              | 5.8    | 0.96                     | 0.98   | 0.55   | Yield at cutoff point |
|                           | 16     | 43.1       | 422.4   | 55.0         | 539.0   | 3.6              | 5.8    | 0.94                     | 1.01   | 0.54   | "                     |
|                           | 17     | 40.2       | 394.0   | 49.4         | 484.1   | 3.5              | 5.4    | 0.93                     | 0.99   | 0.50   | "                     |
|                           | 18     | 24.1       | 236.0   | 30.9         | 302.8   | 4.6              | 6.1    | 0.95                     | 1.07   | 0.60   | "                     |
|                           | 19     | 19.7       | 193.1   | 23.1         | 226.4   | 3.6              | 4.5    | 0.98                     | 1.02   | 0.49   | "                     |
|                           | 20     | 20.8       | 203.8   | 25.7         | 251.9   | 4.0              | 5.0    | 1.03                     | 1.14   | 0.75   | "                     |

Notes ; A trouble occurred during loading for specimen I-9.

Specimen I-1 and II-11 through II-14 were omitted since the specimens were not cut off.

Typical distribution of horizontal displacement for rectangular pier is shown in Fig. 6. As shown in this diagram, the distribution was bent near cutoff point subsequent to  $2\delta_y$ . And, the increase of the angle of displacement followed by the increase of horizontal displacement tended to be greater above cutoff point than below cutoff point.

The vertical displacement was measured at two positions on the upper surface of piers, where the vertical displacement before loading of axial force was zero. Typical relation between the vertical displacement (mean value at two positions) and horizontal displacement is shown in Fig. 7. Even though an axial force was provided, the greater the horizontal displacement became, the more the upper surface of specimen tended to be uplifted. This is considered to be due to the effects of elongation after yield of reinforcement and incomplete touch of the crack faces when cracks was opened and shut at alternate loading.

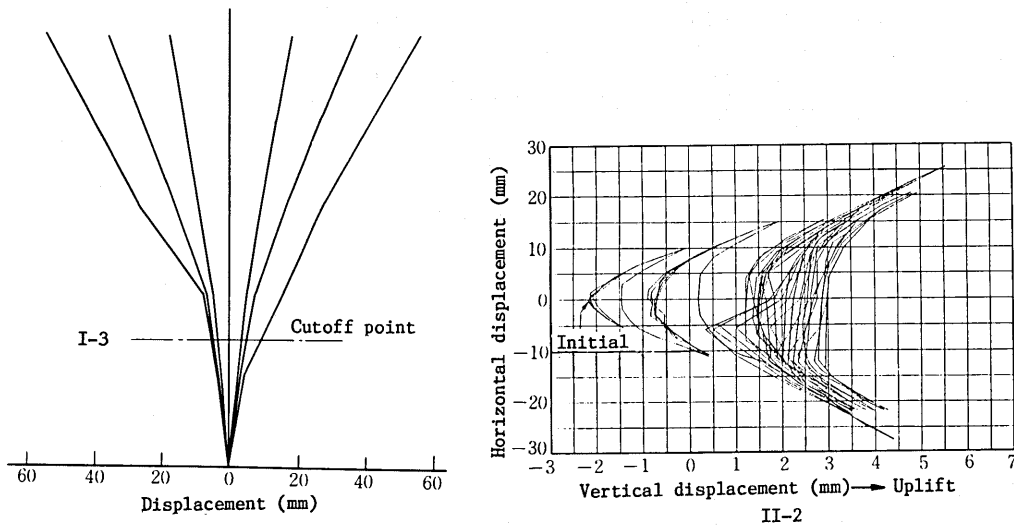
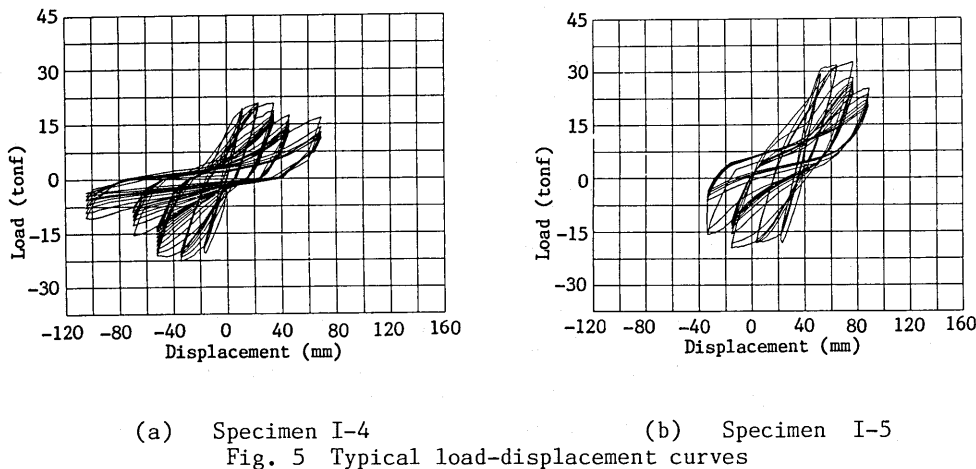
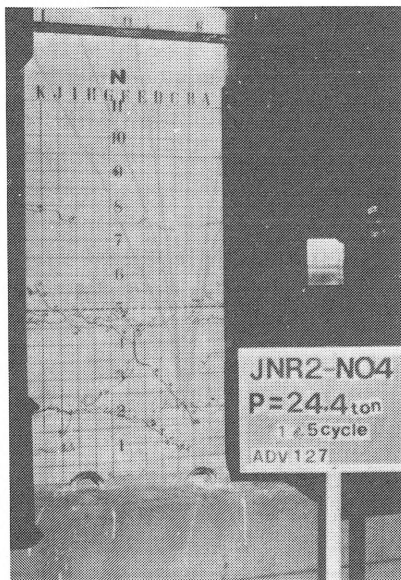


Fig. 6 Distribution of horizontal displacement

Fig. 7 Vertical-horizontal displacement curve

b) Yield load

Table 2 shows the ratio  $P_o/S_y$  of each specimen, where  $P_o$  is a measurement value of flexural yield load of each specimen and  $S_y$  is a calculated value of flexural yield load at cutoff point. The ratio was 0.87 through 1.03 for Series I, 0.69 through 0.93 for Series II, 0.93 through 1.03 for Series III. So that, in most of specimens, tension reinforcement at cutoff point yielded at smaller load than the calculated yield load.

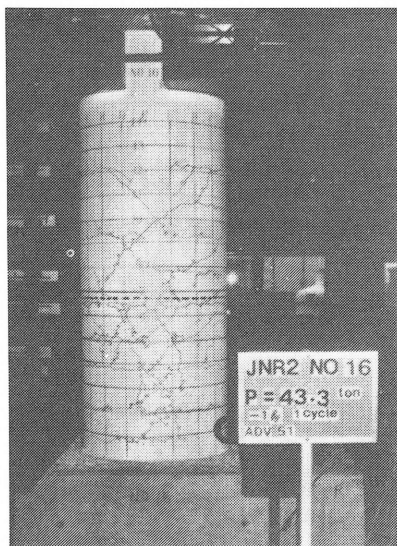


(a) At  $\delta_y$

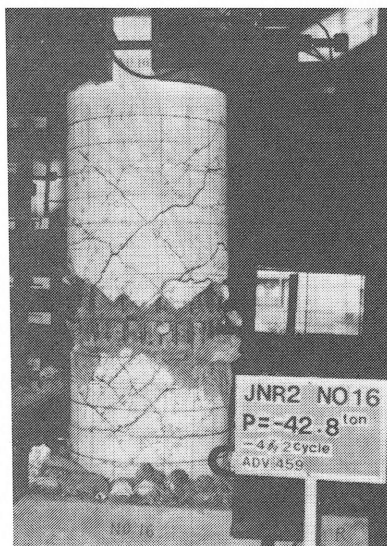


(b) At  $4\delta_y$

Photo 1 Specimen II-4



(a) At  $\delta_y$



(b) At  $4\delta_y$

Photo 2 Specimen III-16

### c) Behavior of cracks and failure

Photo 1 and Photo 2 indicate the typical conditions of cracks and failures in rectangular pier specimens and circular pier specimens.

Initially, cracks occurred on the entire surfaces on the tension side. And then, cracks near cutoff points became predominant and developed into diagonal cracks subsequent to  $2\delta y$ .

For specimen I-11 and I-12, where shear reinforcements were arranged only below cutoff point, diagonal cracks occurred from the shear reinforcement or on the upper side of cutoff point, and the width of crack tended to be expanded. Therefore, shear reinforcements for the other specimens were arranged between a distance  $d$  above and below cutoff point.

Regarding the characteristics of failure, in the case of most of the rectangular pier specimens, bond splitting failure occurred and the concrete cover below cutoff point was peeled off, but such failure seldom occurred in the circular pier specimen. This is considered to be due to the following reasons: Namely, although the tension reinforcement in the circular pier specimen were yielded successively from outside, those in the rectangular pier specimen were yielded at one time. Moreover, in rectangular pier specimen, where the shear reinforcements are of a rectangular form, the confining effect of longitudinal reinforcement and internal concrete is smaller than the confining effect in circular pier specimen.

Meanwhile, there was not observed to be any particularly significant difference in the conditions of cracks on the surfaces of circular pier and rectangular pier respectively at the flexural yield strength.

Remarkable failure characteristics were demonstrated by the specimens of II-3 and II-5, where the amount of shear reinforcement is zero and the acting shear stress at flexural yield strength was comparatively large.

In other words, in these specimens, diagonal cracks occurred at  $\delta y$  displacement level and shear failure occurred subsequent to rapid reduction of resisting strength at  $2\delta y$  displacement level. These diagonal cracks connected in the shape of X from the loading point to the root of pier as shown in Photo 3.

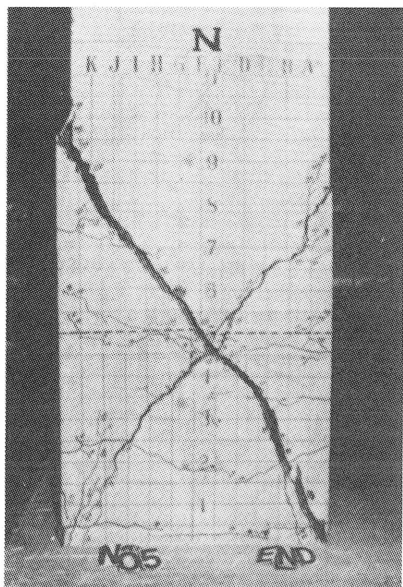


Photo 3 Specimen II-5

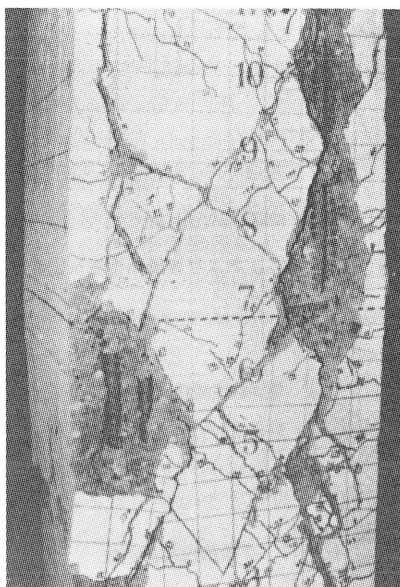


Photo 4 Specimen II-7

Moreover, in the case of the specimen II-7, where ratio of tension reinforcement is as high as 2.02%, bond splitting failure initiated across the overall length of specimen as shown in Photo 4, and its resisting strength was rapidly reduced at  $2\delta_y$  displacement level.

#### d) Effects of cutoff method of reinforcement

In the case of the specimen II-10, its flexural yield strength of the root of specimen was designed nearly equal to that of the cutoff point and its shape was made equal to that of II-9 except in case the cutoff bars at cutoff point were bent rectangularly and terminated inside the specimen. As a result of test, the reinforcement at the root of pier yielded earlier than the reinforcement at cutoff point. Therefore, the test of the specimen II-10 was stopped at that time and the root of specimen was reinforced. The specimen was renamed II-10R as shown in Table 2 and examined again. As a result, in the specimen II-10R, tension reinforcement at cutoff point yielded and the load-displacement curves and ductility factors were similar to those in the case of II-9.

Therefore, in this experiment, it has been clarified that cutoff methods does seldom contribute to the improvement of ductility when tension reinforcement at cutoff point yield even though cutoff bars is bent rectangularly and terminated inside the specimen.

#### e) Distribution of strain in reinforcement

The typical distribution of strain in the longitudinal reinforcement (cutoff bar and non-cutoff bar) at the first peak load at displacement level  $\delta_y$ ,  $2\delta_y$  and  $3\delta_y$  is shown in Fig. 8. The strain distribution curve of non-cutoff bar showed a peak at cutoff point and was decreased due to a mutual action of non-cutoff and cutoff bars as the reference position was gradually taken down from cutoff point. In the case of rectangular pier specimen, both of the strains became nearly equal at the position 20 cm through 30 cm ( $15\phi$  through  $23\phi$ ) below cutoff point.

As the displacement level was increased the more from  $2\delta_y$  to  $3\delta_y$ , the larger the strain in non-cutoff bar became. But the strain of cutoff bar below the cutoff point varied due to the type of specimens. Namely, when the resisting strength was larger than that at the previous displacement level or when the reduction of resisting strength was small, the strain of cutoff bar tended to

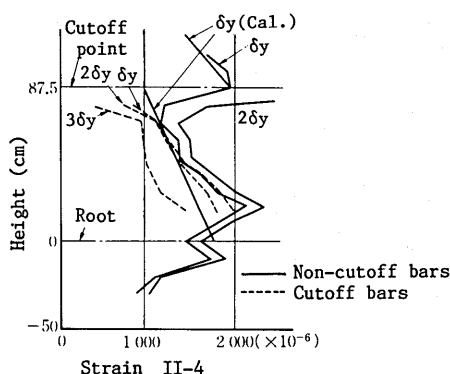


Fig. 8 Distribution of strains in longitudinal reinforcement

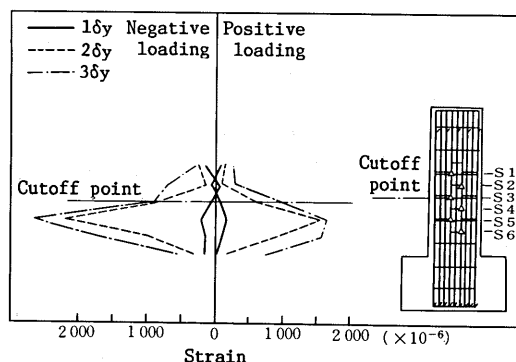


Fig. 9 Distribution of strains in shear reinforcement

increase below the cutoff points. However, when the resisting strength was substantially reduced, the strain of cutoff bar became smaller than that at the previous displacement level. Meanwhile, the strain of the reinforcement at cutoff point had been about  $1900 \times 10^{-6}$  at the  $\delta_y$  displacement level and became  $10000 \times 10^{-6}$  through  $20000 \times 10^{-6}$  at the  $2\delta_y$  displacement level. Fig. 9 shows the strain distributions in shear reinforcement at the first peak load at the displacement levels  $\delta_y$ ,  $2\delta_y$  and  $3\delta_y$ . Each distribution reached a peak near cutoff point and shear reinforcement reached yield at the  $2\delta_y$  displacement level or over.

#### 4. CONSIDERATION

##### (1) Load-displacement envelope curves and equivalent viscous damping factor

Fig. 10 shows typical envelope curves of  $P/P_{max}-\delta/\delta_y$  and typical curves of  $heq-\delta/\delta_y$  for three variables ; cutoff ratio, ratio of shear reinforcement and axial force. Here,  $P_{max}$  is the maximum load of specimen,  $P$  is the maximum value of peak loads at each displacement level  $\delta$ ,  $\delta_y$  is the displacement when the reinforcement of specimen reached yield, and  $heq$  is the equivalent viscous damping factor.<sup>4)</sup> The damping factor  $heq$  was defined by calculating by the equation in Fig. 11. The larger value of this factor means that the dissipation of energy of the specimen is larger. Fig. 10(a) shows a comparison of cutoff ratio 1/2 with cutoff ratio 1/3. There was no difference in the relations between  $P/P_{max}$  and  $\delta/\delta_y$  and between  $heq$  and  $\delta/\delta_y$ . Fig. 10(b) shows a comparison of ratio of shear reinforcement 0 % with 0.17 %. As  $\delta/\delta_y$  becomes larger,  $P/P_{max}$  and  $heq$  in the case of ratio 0.17 % become larger than in the case of ratio 0 %. Moreover, Fig. 10(c) shows a comparison of axial force 0  $kg/cm^2$  with 1.0  $kg/cm^2$  (0.98 MPa). As  $\delta/\delta_y$  becomes larger,  $P/P_{max}$  and  $heq$  in the case of axial force 10  $kg/cm^2$  become slightly smaller than in the case of ratio 0 %.

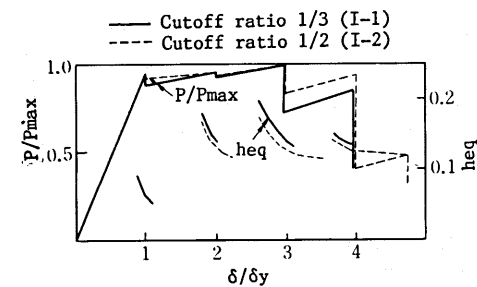


Fig. 10(a) Cutoff ratio 1/2 and 1/3

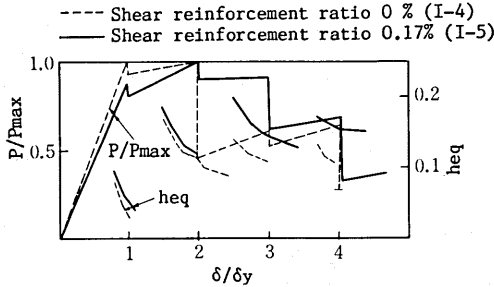


Fig. 10(b) Shear reinforcement ratio 0 % and 0.17 %

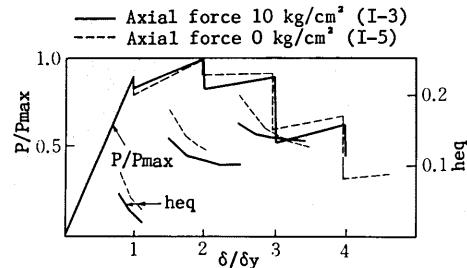


Fig. 10(c) Axial force 0  $kg/cm^2$  and 10  $kg/cm^2$

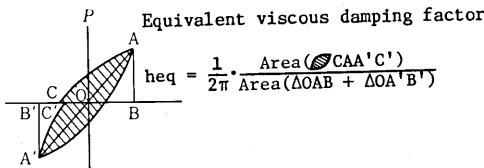


Fig. 11 Equivalent viscous damping factor



## (2) Moment shift length + Development length

"Moment shift" means that the acting force of tension reinforcement at a specified section is balanced against the acting moment at the section which locates at a distance. Namely, the moment at a distance apparently shifts toward the specified section, for example, in the case that diagonal cracks occur and cause shear failure.

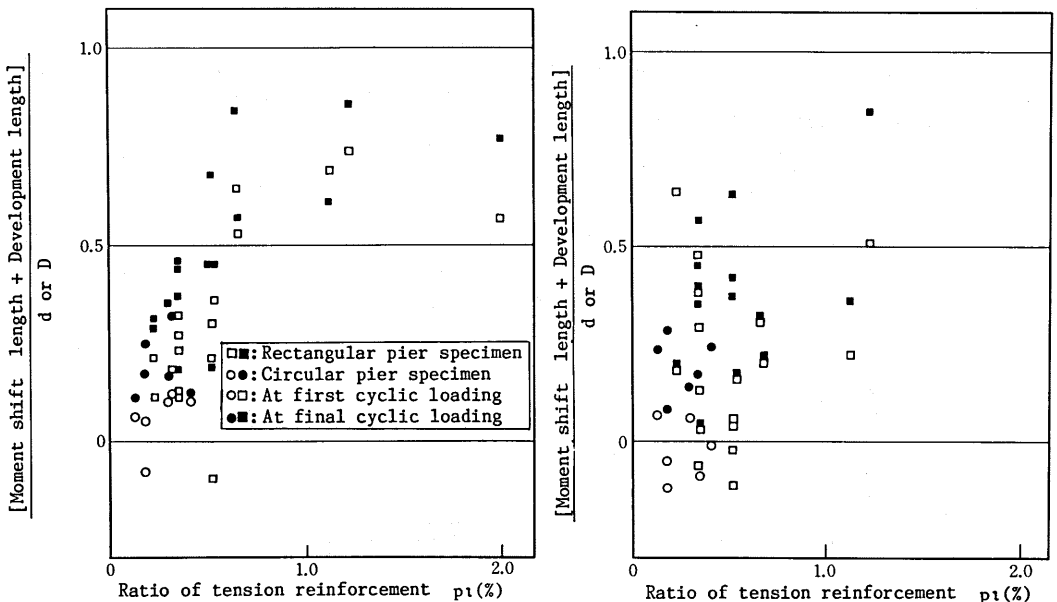
As described in Item 3 (3) b), in this experiment result,  $P_o$  became smaller than  $S_y$ . This is considered to be due to the influences of moment shift and development length of cutoff bar. However, since it is difficult to separate both of the influences, these influences are treated as [Moment shift length + Development length].

[Moment shift length + Development length] was obtained as a distance from cutoff point to the point where the acting moment due to each peak load  $P$  at each displacement level was equal to the flexural yield strength calculated as disregarded cutoff bars. Fig. 12 shows the relation between [Moment shift length + Development length] and ratio of tension reinforcement.

At the  $\delta_y$  displacement level, the higher the ratio of tension reinforcement becomes, the larger [Moment shift length + Development length] tends to become. However, at the  $2\delta_y$ , it seems that the ratio of tension reinforcement does not have so remarkable relationship with [Moment shift length + Development length]. Moreover, there was observed to be no relationship between [Moment shift length + Development length] and  $V_s/S_y$  ( $V_s$ : Shear strength only by shear reinforcing bars) and nor any relationship between [Moment shift length + Development length] and  $M/S_d$ .

## (3) Ductility

### (a) Evaluation method



(a) At  $\delta_y$

(b) At  $2\delta_y$  (in specimens with ductility factor of 2 or more)

Fig. 12 Ratio of tension reinforcement vs. [Moment shift length + Development length]

The ductility at cutoff zone was investigated at the section locating, by wherever the larger value among effective depth  $d$  from cutoff point or the development length, below cutoff point. The ductility factor was evaluated as  $\mu'$ , which was adopted as the smaller value of the factors obtained from positive and negative load-displacement curves shown in Fig.4.

(b) Effect of the ratio  $V_y/Sy'$

Fig.13 shows the relation between the ductility factor  $\mu'$  and  $V_y/Sy'$ . Generally, the ductility factor of reinforced concrete member decreases as  $V_y/Sy'$  becomes smaller. Similarly, in this experiment, the ductility factor  $\mu'$  becomes smaller as  $V_y/Sy'$  becomes smaller. As the correlation between  $\mu'$  and  $V_y/Sy'$  is shown in Fig.13, the following linear regression equation was obtained with the correlation coefficient of 0.7::

$$\mu' = 1.4 (V_y/Sy') + 0.6 \dots\dots\dots(2)$$

For this experiment, the ratio  $a/H$  is in a range of 0.5 to 0.75, where the height  $H$  is the distance from the root to the loading position and the height  $a$  is the distance from cutoff point to the loading position in Fig.2. If the rotation capacity at cutoff point is constant, the ductility factor is theoretically considered to become smaller as the position of cutoff point becomes higher. Namely, the ratio  $a/H$  is smaller and the proportion for which the displacement below cutoff point accounts for the yield displacement become larger since the yield displacement was defined as the horizontal displacement between the root and the loading position when the bars reached yield. But, within  $a/H$  of this experiment, the above trend was not observed. This is considered because the angle of displacement at the position below cutoff point was slightly enlarged due to alternately cyclic loading and because the ductility factor had substantially fluctuated.

c) Effect of  $M/Sd$

Generally, the ductility of reinforced concrete member decreases as the ratio  $M/Sd$  of shear span to effective depth becomes smaller. However, such trend was not observed within the scope of this experiment.

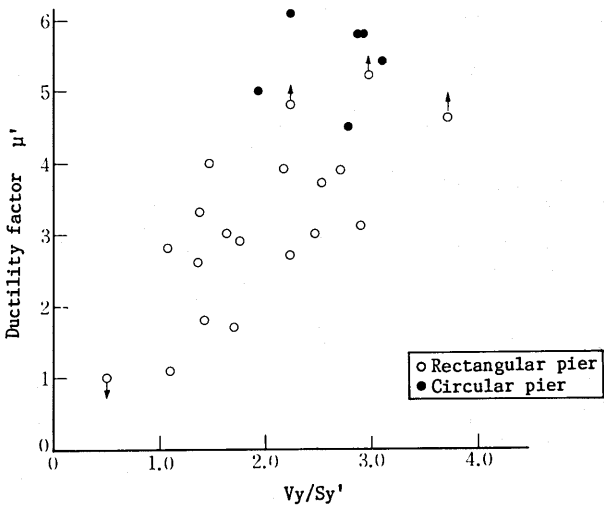


Fig. 13  $V_y/Sy'$  and ductility factor

## 5. SEISMIC DESIGN OF A PIER WITH REINFORCING BARS TERMINATED HALFWAY IN A TENSION ZONE

According to the results of investigating the positions of cutoff points for railway bridge piers, in case the height of piers is about 20 m in maximum, reinforcing bars have been generally cutoff at two points. In most cases, the positions of the first cutoff point have respectively located in a range of 0.5 to 0.75 in  $a/H$  (including the case where reinforcing bars are cutoff at only one position) and the positions of the second cutoff point have been respectively in a range of 0.25 to 0.4 in  $a/H$ . If a pier is exposed above the ground and the reserve load-carrying capacity of cutoff zone has been made larger than that of the root of pier, the reinforcement at cutoff point will not be subjected to yield. However, actually, the root of pier is mostly located under the ground and the resistance of soil is added. So that, there are considered to have been some cases where reinforcement at cutoff point reached yield. According to the results of this experiment, when  $a/H$  is in a range of 0.5 to 0.75 and the cutoff ratio is in a range of  $1/2$  to  $1/3$ , in Eq.(2),  $V_y/S_y'$  should respectively be not less than 1.0 in order to ensure a ductility factor of 2 or more and 1.7 in order to ensure a ductility factor of 3 or more. Moreover, actual load-displacement envelope curves are the same as Fig. 4. Therefore, if the ductility factor calculated by Eq.(2) is used in the design of the piers, as the portion of diagonal lines in Fig. 4 is possible to be taken into account as the reserve load-carrying capacity, and it is considered possible to ensure the safety of pier. If a ductility factor of 3 or more is to be attained, an excessively large amount of reinforcing bars will be required. Therefore, in practicable arrangement of reinforcement, it is considered justifiable to adopt  $V_y/S_y'$  of 1.0 or more and a ductility factor of 2 at cutoff zone for actual pier design. Generally, when a pier yields at its root, it is possible to obtain a ductility factor of about 4. Therefore, where the energy conservation rule is satisfied, it will be necessary to increase as much as fifty percent of the load-carrying capacity of the cutoff zone, in order to attain the earthquake-proof capacity equivalent to the capacity at the root of pier. Where the value at the position C in Fig. 1 is  $4\delta y$ , the following equation is obtained from the relation where Area  $\triangle ABCO$  = Area  $\triangle FGH O$ .

$$r = \sqrt{7 / (2\mu - 1)}$$

When  $\mu = 2$  is substituted into the above equation,  $r = 5$ .

Although the effect of  $a/H$  was not observed within the scope of this experiment, it is considered desirable to further increase the load-carrying capacity of the second or subsequent position of cutoff zones where  $a/H$  is smaller.

In summary, when the portion of longitudinal bars is cut off and terminated halfway in a pier, practicable design methods are recommended to be as presented below.

Where the area of cutoff bars is in a range of  $1/2$  to  $1/3$  of total area of cutoff and non-cutoff bars in the same section, the end of cutoff bars should be located at the larger distance of effective depth or development length from the point of which the flexural strength is not less than 1.5 times the design moment. At the same time, in a range of effective depth above and below cutoff point, the shear strength should be not less than 1.5 times the design shear force. And the shear strength should be obtained by the Eq.(1). Moreover, the second or subsequent cutoff zone should preferably have the larger load-carrying capacity than that at the first cutoff zone.

## 6. SUMMARY

The results of this experiment are summarized as follows.

- (1) The ductility at cutoff zone was smaller than that at the root of pier. As the reason, it is considered that the bond of cutoff bars is lost due to separation of concrete cover after yielding of reinforcing bars at cutoff zone, and the range of damage is extended more.
- (2) Where cutoff ratio is respectively in a range of  $1/2$  through  $1/3$  and  $a/h$  is in a range of  $0.5$  through  $0.75$ , the ductility factor at cutoff zone was roughly proportional to the ratio  $V_y/S_y'$ . Although the ductility factor was expected to become the smaller as  $a/h$  became the smaller, this relationship was not clarified in the result of this experiment.
- (3) On alternate loading at the  $\delta_y$  displacement level, the value of [Moment shift length + Development length] tended to become the larger as ratio of tension reinforcement was the larger.
- (4) In the characteristics of fracture at cutoff zone, there seemed to be no significant difference between cutoff ratio  $1/2$  and cutoff ratio  $1/3$ .
- (5) When the reinforcement at cutoff zone yielded, the equivalent viscous damping factor was roughly  $0.1$ .
- (6) In almost all cases of rectangular piers, the failures at cutoff zone involved bond splitting fractures. In contrast, such bond splitting fractures seldom occurred in the case of circular piers. As the reason, it is considered that the confining effect of shear reinforcement on the longitudinal bars and inner concrete for circular pier was greater than in case of rectangular pier.
- (7) To examine the flexural yield strength at cutoff zone for circular pier, a circle formed by connecting the center of longitudinal bars is taken into consideration. By adopting a value of bending yield strength when the reinforcing bars at a position about one-fourth the diameter of this circle is yielded, the relation between the ductility factor and  $V_y/S_y'$  for circular pier becomes nearly equivalent to that for rectangular pier. Thereby, it is possible to carry out seismic design of circular pier according to nearly equal design procedures for rectangular pier.
- (8) As a result, a seismic design method of pier with reinforcement terminated halfway in a tension zone has been proposed as mentioned in chapter 5.

## ACKNOWLEDGEMENT

The authors wish to express their thanks to Dr. Hajime Okamura, Prof. of Civ. Engrg., Univ. of Tokyo for his valuable advices in compiling this report. Thanks are due also to Mr. Takeji Okada, Institute of Technology, Shimizu Construction Co., Ltd. for much cooperation in conducting this experiment. It is also acknowledged that the subsidy was provided for this experiment by the Yoshida Research Fund.

## REFERENCES:

- 1) Veletsos, A. and Newmark, N.M. ; "Effect of inelastic behavior on the response of simple systems to earthquake motions", Proc. 2nd WCEE, 1960.
- 2) Japan Society of Civil Engineers ; "Standards and Commentary for Structural Design of the Japanese National Railways (JNR) (Reinforced concrete structures and plain concrete structures)", 1983.
- 3) Japan Society of Civil Engineers ; "Proposal for Limit States Design of Concrete Structures", Concrete Library, No.48, April, 1981.
- 4) Architectural Institute of Japan ; "Data Book of Seismic Design for Buildings", 1981.